Proceedings of the 5th International Conference on Nonlinear Dynamics
ND-KhPI2016
September 27-30, 2016, Kharkov, Ukraine

Nonlinear Vibrations of Rotors in Systems with Magnetic Bearings

Gennadii Yu. Martynenko [1]

Abstract
A method is suggested for building mathematical models of dynamics of rotors in magnetic bearings of different types (passive and active ones). It is based on Lagrange-Maxwell differential equations in a form identical to that of Routh equations in mechanics. The main distinguishing feature of the model is the possibility to account for the following: the nonlinear dependence of magnetic forces on gaps between movable and stationary parts in PMBs and AMBs, and on currents in the windings of AMB electromagnets; current delay in the windings of AMB electromagnets, i.e. nonlinearity linked to the inductance of the coils; the geometric links between the electromagnets of one AMB and the links between all AMB of one rotor, which results in coupling of processes in orthogonal directions; practically any AMB control law; limitations on the control current caused by physical constraints in the control system controller; dissipation fluxes as well as magnetic resistances of AMB magnetic core sections, making the mathematical model insensitive as regards origination of "nonzero" gaps and currents. Numerical analysis has been performed for one of the possible variants of a complete rotor magnetic suspension realised in the form of the laboratory model. It includes two radial passive magnetic bearings with permanent annular magnets and one axial active magnetic bearing with a stator in the form of a shell core. Modelling validity is confirmed by comparing analytical and experimental data. Analysis of linear and nonlinear rotor dynamics phenomena observed in the laboratory model with magnetic bearings is described It is known that analysis based on linearised models allows judging only the stability of equilibrium states with small deflections. The negligible nonlinear equation terms in this case, when investigating motion with increasing deflection, allow expanding the information content of the mathematical model about nonlinear effects occurring in the system. Estimated results revealed shortcomings of the linearised models. Based on this conclusion the need of using nonlinear models for adequate description of the dynamics of such systems is proved

Keywords
rotor dynamics, magnetic bearings, mathematical model, Lagrange-Maxwell differential equations, nonlinear vibrations

[1] National Technical University “Kharkiv Polytechnic Institute”, Kharkiv, Ukraine
*** Corresponding author:** gmartynenko@ukr.net

Introduction

A magnetic bearing (MB) is a design variant of elastic-damping bearings. Its feature is the use of magnetic fields to provide stable rotor levitation. These fields create bearing force responses to rotor displacement in order to ensure automatic alignment of its bearing areas in the MB stator elements and a required level of bearing stiffness. MBs that are the most applicable from the practical viewpoint are active magnetic bearings (AMBs) [1-5] and passive magnetic bearings (PMBs) [6].

Based on the opportunities of practical implementation of complete rotor magnetic bearings, this study considers the options of using either radial or axial AMBs for stabilising a rotor over all five degrees of freedom or one AMB jointly with several PMBs in different design versions. The most practical approach would be to use a combination of magnetic bearings of different types in medium-sized high-speed rotor machinery, e.g., turbo-expanders, and expander-generator and expander-compressor units [4]. They can use two radial PMBs and one axial AMB arranged in the centre or at one end of the shaft. This is due to the design features such as the presence of one or two discs arranged on the rotor cantilevers [7].

In considering the problem of describing the dynamics of rotors in different power machinery in which magnetic bearings are used as rotor bearing assemblies, a conclusion can be made on the

need to develop special approaches to mathematical modelling with account for all specific features that this kind of elastic damping bearing introduces into rotor systems. Presently, there is a large variety of studies on this subject. However, they offer a simplified linear approach to mathematical modelling of rotor dynamics. However, rotor systems with nonlinear bearings, including magnetic ones, are known to exhibit nonlinear effects [8, 9]. Therefore, building refined mathematical models will enable increasing the accuracy of numerical computation of required dynamic parameters of rotors, magnetic bearings and control systems for active magnetic bearings. This will dramatically reduce the amount of experimental investigations and increase the effectiveness of research and development efforts.

The objective of this study is a practical implementation of the method for substantiating the need to use nonlinear mathematical models for describing the dynamics of rotor systems with MB.

1. Mathematical model of rotor dynamics in a laboratory setup

The dynamic behaviour of a rotor in an MB was analysed for a laboratory setup of a rotor in a complete combined passive-active magnetic suspension, which was a prototype of the magnetic suspension for a rotor in an expander compressor unit (ECU). A schematic diagram of a complete magnetic suspension of a rotor, including two radial PMB1,2 and one axial AMB3, is shown in Fig. 1. A detailed description of the laboratory setup and of the PMB and AMB is given in [10]. A rigid rotor is considered because the vibrations caused by dynamic unbalance induce motion of the cylindrical and conical precession type. They are the most common ones in practice and are distinguished by excessive amplitudes, making them especially dangerous.

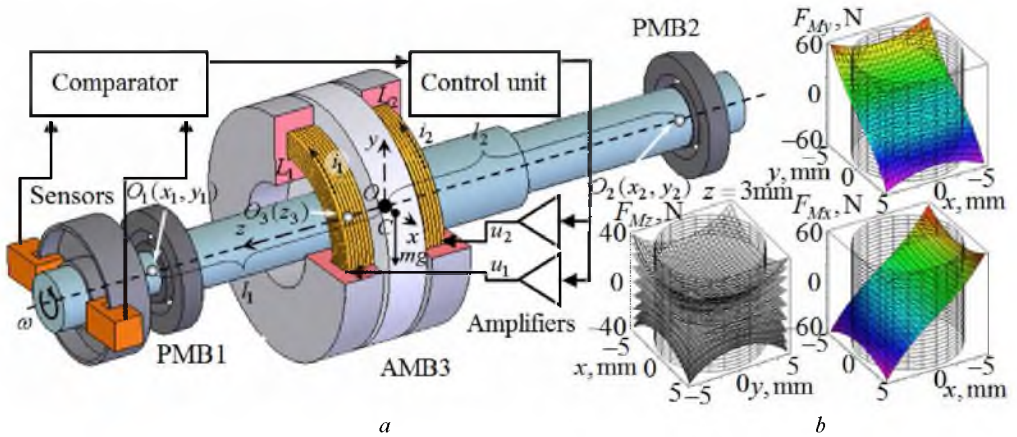

a *b*

Figure 1. Complete suspension for a laboratory setup rotor in an MB: *a* – schematic diagram; *b* – restoring magnetic forces in PMB1 and 2 vs. rotor displacements

If the energy of the AMB3 magnetic field is $W=W(x_1,y_1,x_2,y_2,z_3,\Psi_{c1},\Psi_{c2})$, then the currents in the windings of its coils i_{c1} and i_{c2} are linked to total magnetic fluxes through the circuits of coils Ψ_{c1}, Ψ_{c2} (flux linkage in windings of respective AMB3 electromagnets) by the following expressions:

$$i_{c1} = \frac{\partial W(x_1, y_1, x_2, y_2, z_3, \Psi_{c1}, \Psi_{c2})}{\partial \Psi_{c1}}, \quad i_{c2} = \frac{\partial W(x_1, y_1, x_2, y_2, z_3, \Psi_{c1}, \Psi_{c2})}{\partial \Psi_{c2}} . \tag{1}$$

We also assume that all generalised coordinates – displacements $x_1,...,z_3$, unbalance parameters e_1, e_2 and γ_1, γ_2, and gaps in the MB – δ_{r1}, δ_{r2}, and δ_a – have the same order of smallness. Then, with account for this assumption on smallness of generalised coordinates and their derivatives, the nonlinear addends of equations of motion can be considered small as compared to the linear terms. By excluding from consideration the addends of the equations of motion, with an order of smallness higher than three, we derive a completely coupled system of seven nonlinear differential equations describing the dynamics of this electromagnetic mechanical system:

$$\begin{cases} m_{11}\ddot{x}_1 + m_{12}\ddot{x}_2 + j(\dot{y}_1 - \dot{y}_2) + f''_{x1} + f'''_{x1} + b_{x1}\dot{x}_1 = F_{Mx1}(x_1, y_1) - \dfrac{\partial W}{\partial x_1} + Q_{x1} + H_{x1}(t); \\ m_{22}\ddot{x}_2 + m_{12}\ddot{x}_1 - j(\dot{y}_1 - \dot{y}_2) + f''_{x2} + f'''_{x2} + b_{x2}\dot{x}_2 = F_{My1}(x_1, y_1) - \dfrac{\partial W}{\partial x_2} + Q_{x2} + H_{x2}(t); \\ m_{11}\ddot{y}_1 + m_{12}\ddot{y}_2 - j(\dot{x}_1 - \dot{x}_2) + f''_{y1} + f'''_{y1} + b_{y1}\dot{y}_1 = F_{Mx2}(x_2, y_2) - \dfrac{\partial W}{\partial y_1} + Q_{y1} + H_{y1}(t); \\ m_{22}\ddot{y}_2 + m_{12}\ddot{y}_1 + j(\dot{x}_1 - \dot{x}_2) + f''_{y2} + f'''_{y2} + b_{y2}\dot{y}_2 = F_{My2}(x_2, y_2) - \dfrac{\partial W}{\partial y_2} + Q_{y2} + H_{y2}(t); \\ m\ddot{z}_3 + f''_{z3} + f'''_{z3} + b_{z3}\dot{z}_3 = F_{Mz3}(x_1, y_1, z_1) + F_{Mz3}(x_2, y_2, z_2) - \dfrac{\partial W}{\partial z_3} + Q_{z_3} + H_{z_3}(t); \\ \dot{\Psi}_{c1} + r_{c1}\dfrac{\partial W}{\partial \Psi_{c1}} = u_{c1}(x_1, x_2, y_1, y_2, z_3); \qquad \dot{\Psi}_{c2} + r_{c2}\dfrac{\partial W}{\partial \Psi_{c2}} = u_{c2}(x_1, x_2, y_1, y_2, z_3); \end{cases} \tag{2}$$

where $f''_{qr}(x_1,...,z_3)$ and $f'''_{qr}(x_1,...,z_3)$ are nonlinear terms of the equations of motion due to inertia forces and the second and third-order potential field; $b_{x1,...,z3}$ are viscosity coefficients; $r_{c\,1,2}$ are active resistances in winding circuits; $u_{c\,1,2}$ are control voltages applied across AMB windings whose magnitude is formed according to the accepted control law depending on the rotor current position; m_{ks}, j are inertial and gyroscopic coefficients with the following values:

$$m_{11} = \frac{ml_2^2 + J_1}{l^2};\ m_{12} = \frac{ml_1l_2 - J_1}{l^2};\ m_{22} = \frac{ml_1^2 + J_1}{l^2};\ j = \frac{\omega J_3}{l^2}. \tag{3}$$

Addenda F_{Mqr} are potential forces that depend only on the generalised coordinates. In this case, these are the magnetic forces in PMB1,2 (Fig. 1, b). The magnetic forces dependencies were obtained using the Maxwell tension tensor by solving a series of magnetic statics problems in the finite element statement for a fixed number of rotor magnet positions corresponding to certain discrete values of its displacement, though they can be described by analytical expressions as in [11]. Terms $-\partial W/\partial q_r$ are ponderomotive forces, i.e. the electromagnetic responses of AMB3. Their dependence on the generalised coordinates and currents in windings is suggested in this study to be obtained analytically by considering magnetic circuits with the use of equivalent circuits and the loop fluxes method [12]. Forces Q_{qr} are other generalised forces, in particular, the force of gravity, and $H_{qr}(t)$ are external time-dependent exciting forces and moments, in particular, caused by unbalance:

$$\begin{cases} H_{x1}(t) = m_{11}\mathrm{E}_x + j\Gamma_x;\ H_{x2}(t) = m_{22}\mathrm{E}_x - j\Gamma_x; \\ H_{y1}(t) = m_{11}\mathrm{E}_y - j\Gamma_y;\ H_{y2}(t) = m_{22}\mathrm{E}_y + j\Gamma_y; \\ \mathrm{E}_x = e_1\cos(\omega t) - e_2\sin(\omega t);\ \mathrm{E}_y = e_1\sin(\omega t) + e_2\cos(\omega t); \\ \Gamma_x = \gamma_1\sin(\omega t) + \gamma_2\cos(\omega t);\ \Gamma_y = \gamma_1\cos(\omega t) - \gamma_2\sin(\omega t). \end{cases} \tag{4}$$

Second-order nonlinear terms $f''_{qr}(x_1,...,z_3)$ and third-order nonlinear terms $f'''_{qr}(x_1,...,z_3)$ are not shown here due to their cumbersome notation; however, it is these terms that demonstrate the full co-relation between all generalised coordinates with the help of terms independent of unbalance parameters [10].

A detailed technique for deriving system of equations (2) and all terms and expressions for magnetic energy for an axial AMB3, depending on flux linkages $\mathbf{\Psi}=\{\Psi_{c1},\Psi_{c2}\}$ and generalised coordinates $\mathbf{q}=\{x_1,y_1,x_2,y_2,z_3\}$, is described in [10]. A final expression for magnetic energy in terms of flux linkage and generalised mechanical coordinates:

$$W(\mathbf{q},\mathbf{\Psi}) = \frac{1}{2}\left[\frac{R_{\Psi 11}(\mathbf{q})}{w_1^2}\Psi_{c1}^2 + \frac{R_{\Psi 22}(\mathbf{q})}{w_2^2}\Psi_{c2}^2 + \frac{R_{\Psi 12}(\mathbf{q})}{w_1 w_2}\Psi_{c1}\Psi_{c2}\right]. \tag{5}$$

Constituent in coefficients R_Ψ, the magnetic resistances of magnetic core sections R_{pk} R_{sk}, R_{lk}

and of the disk R_{ak} are constant values depending on the geometric and physical parameters of AMB, and they can be found using schematisation of magnetic flux paths [12]. The dependence of coefficients R_Ψ in the magnetic energy expression (5) on generalised coordinates **q** is determined by the dependence thereon of the resistances of air gaps between the poles and the rotor $R_{gk}(x_1,y_1,x_2,y_2,z_3)$.

Magnetic energy expression (5) is used in system of equations (2) in all equations. Term $-\partial W/\partial z_3$ in the fifth equation describes the axial force, and terms $-\partial W/\partial x_1$, $-\partial W/\partial x_2$, $-\partial W/\partial y_1$, $-\partial W/\partial y_2$ in the first four equations describe radial forces created by the axial AMB3 when the rotor is in an arbitrary position. Terms $-\partial W/\partial \Psi_{c1,2}$ according to (1) are currents in the windings of AMB3 electromagnets.

2. Experimental research

Research was conducted for a rotor with a mass of 2.5 kg in a complete magnetic-electromagnetic suspension (Fig. 1), in which, for AMB3, a unique control method and an algorithm were used, i.e. formation of $u_{c\,k}$ in (2) [13 and 14]: $u_{c2,1}=(u_{\max}-2u_{\min})z_3^2/(2\delta_a^2)\pm u_{\max}z_3/(2\delta_a)+u_{\min}$. The basic parameters have the following values: l_1=0.118 m; l_2=0.166 m; J_1=0.00997 kg·m^2; J_3=0.00347 kg·m^2; $\delta_r=5.5\cdot10^{-3}$ m; $\delta_r=3\cdot10^{-3}$ m; $e=6\cdot10^{-5}$ m; γ=0.003 rad; $u_{\max}$=24 V, and $Q_{Rqr}=b_{qr}\cdot\partial q_r/\partial t$, where b_{qr}=2.325 kg/s. A laboratory setup with such parameters was developed as a prototype of a complete magnetic suspension for an ECU rotor. It was used for experimental studying of possible nonlinear dynamic phenomena in the system when the angular rotational speed changes within 0 to 3 000 rpm.

The result of a series of experiments was the amplitude-frequency response (AFR) shown in Fig. 2. It allows evaluating the presence of resonant modes in the area being investigated and the kind of rotor motion corresponding to different rotational speeds. Thus, the following was found:

– bifurcation of the first (~10.5 and ~12 Hz) and the second (~22.5 and ~33 Hz) resonances due to different PMB stiffness in the horizontal and vertical directions (anisotropy of bearings) due to different static equilibrium positions ($x_{1st}=x_{2st}=0$, y_{1st} and $y_{2st}\neq0$) with respect to centres of bearings that occur owing to the force of gravity;

– direct (<10.5 Hz) and reverse (<12 Hz) cylindrical precessions as well as direct (<22.5 Hz) and reverse (<36 Hz) conical precessions (Fig. 2, a shows vibration modes corresponding to these motions);

– loss of vibrations with transition from one stable mode to another stable mode (in Fig. 2, the crosshatched area within ~31-38 Hz is that of unstable motion, in which the vibration amplitudes, without introducing extra mechanical damping, exceed the PMB radial gap).

Besides, our analysis of the results detected in the system concerned the following: harmonic vibrations with an excitation (rotational) frequency, sub and superharmonic vibrations, multiple sub and super resonances, and a link between radial and axial vibrations. A detailed description of the results is given in the following, in comparison with the results of numerical modelling.

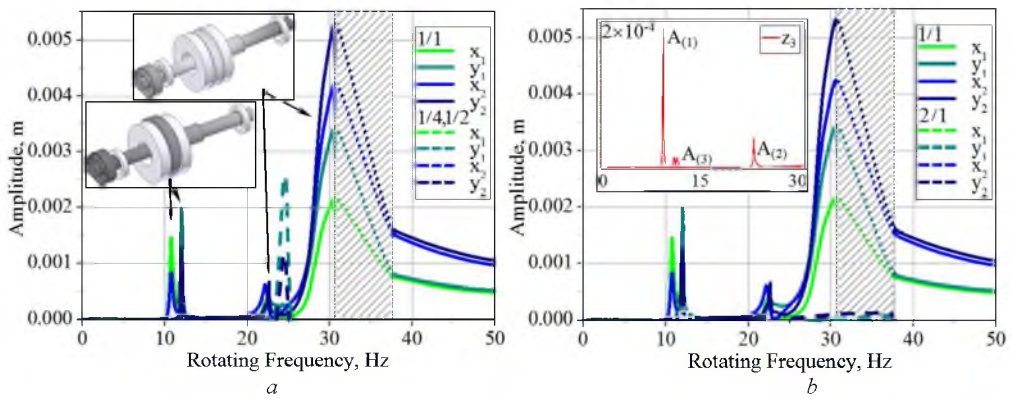

Figure 2. Experimental AFR response of the rotor and amplitude vs. rotational frequency response: *a* – subharmonics; *b* – superharmonics

3. Numerical research

The parameters of the natural vibrations of the stiff rotor were computed using a linearised system of equations without account of damping. The eigen modes (EM) and their respective natural frequencies (NF) are shown in Fig. 3a. In spite of the axial symmetry of the MBPRM force characteristics, the values of both first NF p_{1x}, p_{1y} and second NF p_{2x}, p_{2y} are different because the stiffness values in MBPRM1 and 2 along x and y were computed for static equilibrium of the rotor with account of the force of gravity (shown in Fig. 3a with dashed lines in absolute units). The first (no-node) and the second (with no node) EM in both directions are identical. From the rotor dynamics viewpoint they correspond to cylindrical and conical precessions. Building the frequency (Campbell) diagram (Fig. 3b) calculated with account of the dependence of natural frequencies on rotor angular speed ω, i.e. with account of the gyroscopic effect, allowed specifying the values of critical frequencies ω_{1x}, ω_{1y} and ω_{2x}, ω_{2y} corresponding to cylindrical and conical precession. It was found that at $\omega_{1x}<\omega<\omega_{1y}$ и $\omega_{2x}<\omega<\omega_{2y}$ rotor unbalance causes reverse precession, and with other values of ω it results in direct precession. Computational (natural frequencies – NF and critical frequencies – CF) and experimental (resonance frequencies – RF) data are shown in Table 1.

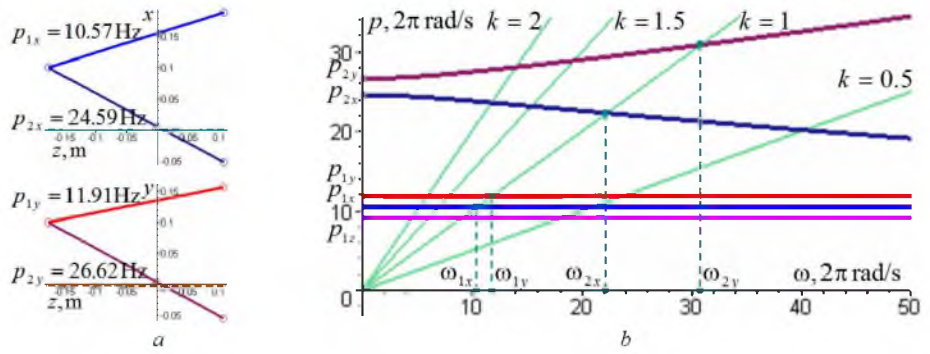

Figure 3. Results of linear analysis of rotor dynamics: *a* – natural frequencies and eigen modes of a non-rotating rotor; *b* – Campbell resonance diagram

Table 1. Comparison of computational and experimental results

Rotor motion kind	Precession direction	Computational		Experimental	Discrepancy, %	
		NF, Hz / rad/s	CF, Hz / rad/s	RF, Hz / rad/s		
Axial vibrations		9.21 / 57.87	9.2 / 57.81	9.5 / 59.7	3.1	3.2
Cylindrical precessions	Reverse	10.57 / 66.41	10.55 / 66.29	10.5 / 66.0	0.7	0.5
	Direct	11.91 / 74.83	11.92 / 74.77	12.0 / 75.4	0.8	0.7
Conical precessions	Reverse	24.59 / 154.50	22.3 / 140.1	22.5 / 141.4	9.3	0.9
	Direct	26.62 / 167.26	30.9 / 194.2	33.0 / 207.3	19.3	6.4

Several factors determine the discrepancy of both the values and critical speeds calculated for the natural frequencies of flexural modes without account of rotor speed and of the critical speeds obtained with account of the gyroscopic moment by the Campbell diagram with definite experimental resonance frequencies. First, the impact of resistance forces decreases the values of resonance frequencies (critical speeds), and second, the nonlinear stiff force charactersitic of the MBPRM (Fig. 1b) increases these values as compared to constant stiffness coefficients of the MBPRM used in linear analysis. In this case, obtaining more accurate resonance frequency values and investigating sub and superharmonic vibrations is possible only with application of a complete nonlinear mathematical model (2).

During numerical modelling, the system of equations (2) was solved with the 4^{th}-5^{th}-order Runge-Kutta method for discrete angular speed values. The many-valuedness of the solution was checked and excluded by multiple computations for each frequency and different initial conditions. In doing so, stationary areas were searched for, whereas time intervals corresponding to transient processes were excluded from consideration. Hence, the results of the numerical analysis of forced vibrations are solutions for stationary areas and generalised coordinates x_1, y_1, x_2, and y_2 in the angular

speed range of 0-100π rad/s. They are shown in Figs. 4 and 5 as harmonics amplitudes A obtained by using the fast Fourier transform versus the driving force angular frequency ω_0 caused by the rotor's own unbalance. This frequency relates to the rotor angular speed as $\omega_0=\omega$.

Computational data were used to determine the values of resonance frequencies [Hz]: ω_{1z}=9.5, ω_{1x}=10.5, ω_{1y}=12, ω_{2x}=22.5, ω_{2y}=36 (failure), which are a close fit to experimental data (Table 1).

Fig. 4 shows the results of computation of rotor forced vibrations caused by dynamic unbalance. The results of order analysis are shown as a spectrogram of generalised coordinates, where: f is spectral frequency, ω is angular speed (rotational frequency), A is amplitude of respective generalised coordinate.

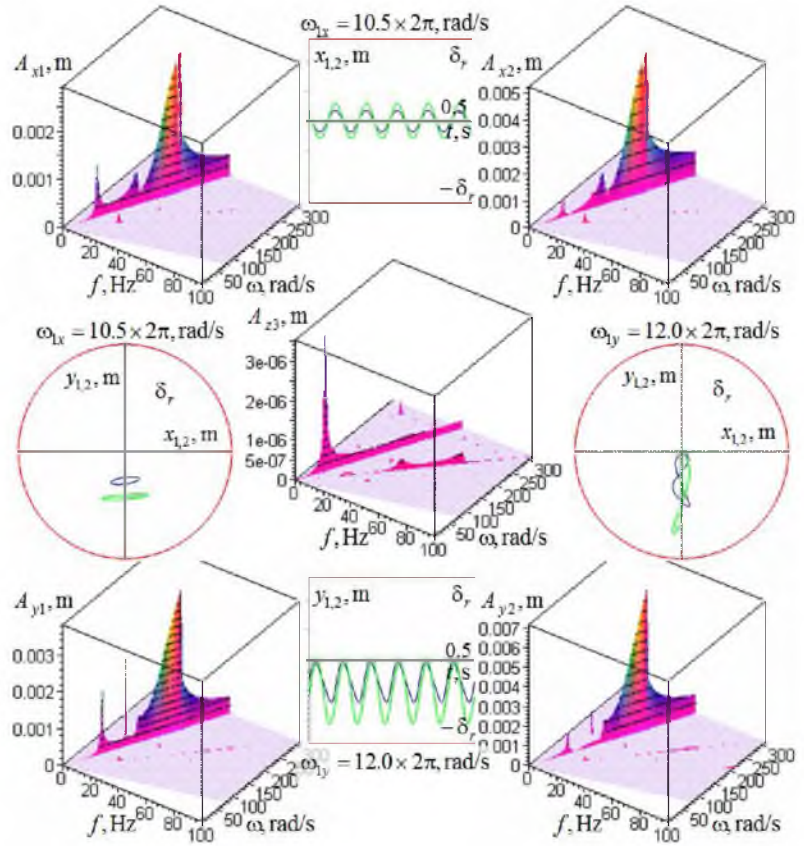

Figure 4. Results of order analysis of rotor motion vibrograms along generalised coordinates within the rotational frequency range of 0-100π rad/s with FFT harmonics expansion

The following notations are used in Fig. 5: $A_{(1)}$ is first harmonic amplitude (Fig. 5), $A_{(1/n)}$ is subharmonic amplitude (Fig. 5, a and c) and $A_{(n)}$ is superharmonic amplitude (Fig. 5, b and d), where the number in parentheses is the multiplicity of the harmonic frequency with respect to the natural frequency ω_0, with the dashed lines showing the skeleton curves. The curves in Fig. 5 show the dynamic behaviour of a rotor in the investigated range and, in essence, they are the projections of 3-dimensional spectra on the coordinate planes $O\omega A$. Thereat, the dependence of the amplitude of the first harmonic of forced vibrations $A_{(1)}$ on the frequency of the harmonic driving force is the amplitude-frequency response, and the graphic representation of this dependence (Fig. 5) is the resonance curve. Analysis of these responses has shown that the first resonant mode (ω_{1z}) corresponds to axial vibrations.

Next, analysis of the results (Fig. 5) has demonstrated the following: superharmonic vibrations in the area of the second resonant mode (I); bifurcation of the second resonance due to anisotropy of PMB stiffness in the horizontal and vertical directions when at $\omega<\omega_{1x}$ and $\omega>\omega_{1y}$ the rotor's motion is of the direct cylindrical precession type, and in the range between these critical speeds $\omega_{1x}<\omega<\omega_{1y}$ the

motion is of the reverse cylindrical precession type (II); super-resonant vibrations $\omega_{2x(2)}$, which coincide also with the inner resonance $\omega_{2x(2)}=\omega_{1y}$ (III); bifurcation of the third resonance due to anisotropy of PMB stiffness when at $\omega<\omega_{2x}$ and $\omega>\omega_{2y}$ rotor motion is of the direct conical precession type, and in the range between these critical speeds ($\omega_{2x}<\omega<\omega_{2y}$) when the motion is of the reverse conical precession type (IV); external resonance $\omega_{1x}+\omega_{1y}\approx\omega_0$ (V); subresonance vibrations $\omega_{1y(1/2)}$ amplified by inner resonance $\omega_{1y(1/2)}=2\omega_{1y}=2\omega_{2x(2)}$ (Fig. 5), with these subharmonic vibrations occurring at relatively big excitation frequencies and their amplitudes significantly exceeding the amplitudes of the first harmonic (VI); the form of resonance curves in the area of the third resonant mode (ω_{2x} and ω_{2y}) is specific to systems with rigid characteristics of the restoring force, which is true for PMB (VII); the third resonant mode is more dangerous than the second one because it is accompanied by a significant amplitude increase because during motion of the conical precession type (angular vibrations) the flatness of gaps in the axial AMB is disturbed, resulting in a moment coinciding with the angular deflection direction of the rotor (VIII); in the area of frequencies, wherein two stable forced vibration modes with two different amplitudes are possible, a failure of vibrations is observed (IX); the fundamental and the superharmonic resonant vibrations in the axial direction are excited by a load acting in the radial direction (by the rotor's own unbalance), with the peaks of super-resonant axial vibrations coinciding with the peaks of the fundamental radial vibrations (Fig. 5, c, d and a, b), which is the result of accounting for the interrelation between radial and axial generalised coordinates with nonlinear terms in the equations of motion (2) (X).

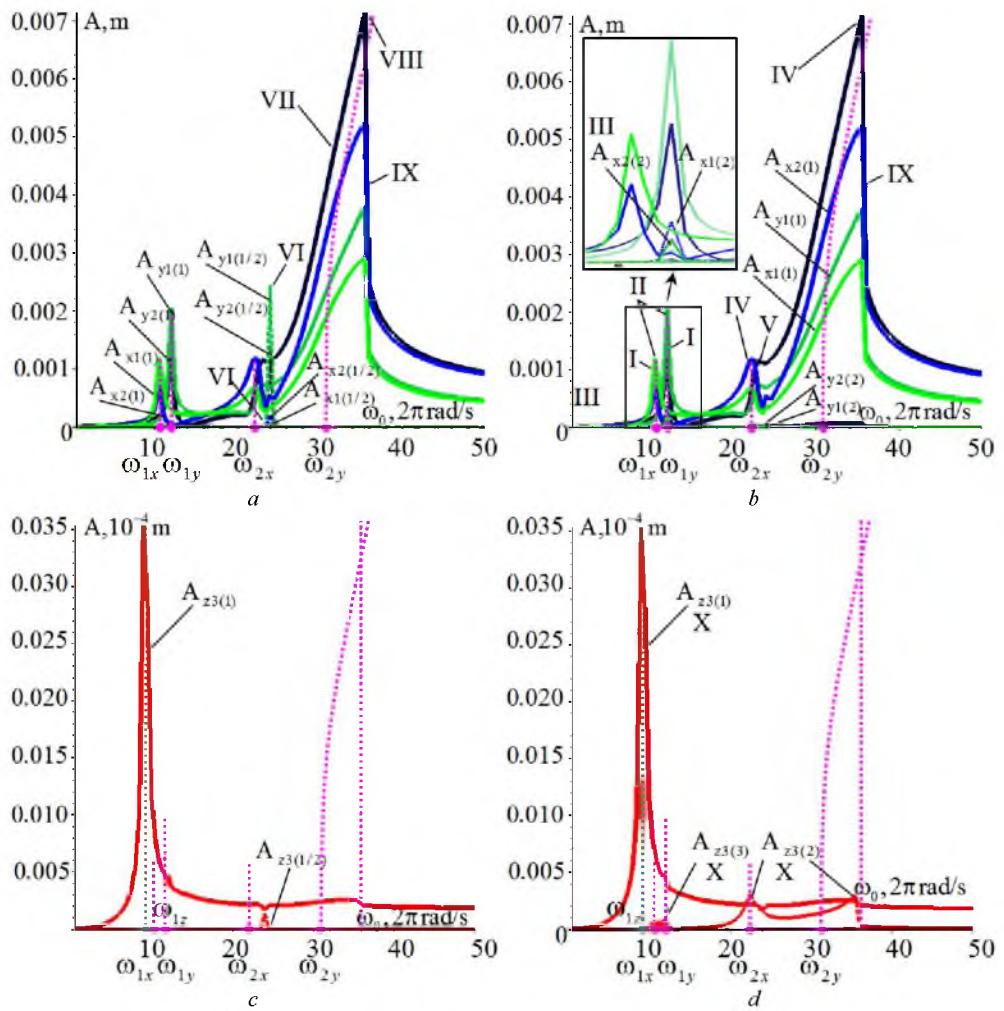

Figure 5. Amplitudes of fundamental, sub and superharmonics vs. driving force frequency: *a*, *b* – x_1y_1,x_2y_2; *c*, *d* – z_3

The same resonant modes and phenomena were found in the system also during experimental research. The adequacy of the mathematical model representing a system of nonlinear completely mutually coupled by generalised mechanical coordinates $x_1,...,z_3$ and flux linkages Ψ_{c1} and Ψ_{c2} equations (with account for the control law, i.e. voltages $u_{1,2}$ also dependent on $x_1,...,z_3$) can be judged by the results of comparing the calculated data (Fig. 5) with experimentally obtained amplitude-frequency responses (Fig. 2) and dependencies of harmonic amplitudes that differ from the fundamental one by the driving force frequency. Thus, comparative analysis of the results has shown an identity for both qualitative representation of processes in the system and quantitative determination of their parameters: for the amplitude, the difference is within 2-3 %, and for the values of resonant frequencies, the difference is within <0.1 %.

Conclusions

The result of this research, which is a follow-up of a large variety of studies, is the development and practical implementation of the method of mathematical description of linear and nonlinear rotor dynamics phenomena in systems with magnetic bearings of different types, which affect the vibration activity of power rotor machinery. The advantage of the approach suggested is that the interrelationship of electric, magnetic and mechanical stationary and nonstationary processes can be accounted for as shown by the example of a laboratory setup. It is shown that linearised models and linear approaches to investigating processes in rotor systems with MB rule out the description of the entire gamut of rotor dynamics phenomena such as sub and super-resonances, though they can present a greater hazard than fundamental ones do.

References

[1] Schweitzer G., Bleuler H., Traxler A. *Active magnetic bearings*. Zurich; ETH; 1994.

[2] Maslen E.H. *Magnetic Bearings*. Charlottesville: University of Virginia Department of Mechanical, Aerospace, and Nuclear Engineering; 2000

[3] Schweitzer G.; Gupta K. (Ed.). Applications and Research Topics for Active Magnetic Bearings. *IUTAM Bookseries*, 2011. p. 263-273. doi: 10.1007/978-94-007-0020-8_23

[4] Schweitzer G., Maslen E. H. (Eds.) *Magnetic Bearings. Theory, Design, and Application to Rotating Machinery*. Berlin: Springer; 2009. doi: 10.1007/978-3-642-00497-1

[5] Polajžer, B. (Ed.). *Magnetic Bearings. Theory and Applications*. Rijeka: Sciyo; 2010.

[6] Jansen R., DiRusso E. *Passive Magnetic Beating With Ferrofluid Stabilization*. Cleveland: Lewes Research Center; 1996.

[7] Simms J. *Fundamentals of the Turboexpander: Basic Theory and Design*. Santa Maria: Gas Technology Services; 2009.

[8] Ji J.C., Hansen C.H., Zander A.C. *Nonlinear Dynamics of Magnetic Bearing Systems*. Journal of Intelligent Material Systems and Structures, 2008, Vol. 19 (12), p. 1471-1491.

[9] Ehrich F.F. Observations of Nonlinear Phenomena in Rotordynamics. Journal of System Design and Dynamics, 2008, Vol. 2 (3), p. 641-651. doi: 10.1299/jsdd.2.641

[10] Martynenko, G. *The Interrelated Modelling Method of the Nonlinear Dynamics of Rigid Rotors in Passive and Active Magnetic Bearings*. Eastern-European Journal of Enterprise Technologies, 2016, Vol 2/5(80). doi: 10.15587/1729-4061.2016.65440

[11] Bekinal S.I., Anil T.R.R., Jana S. *Analysis of radial magnetized permanent magnet bearing characteristics*. Progress In Electromagnetics Research B, 2013, Vol. 47, p. 87-105. doi: 10.2528/pierb12102005

[12] Martynenko G. Modeling the Dynamics of a Rigid Rotor in Active Magnetic Bearings. In: *6th EUROMECH Nonlinear Dynamics Conference (ENOC2008), Proceedings, June 30-July 4, 2008, St. Petersburg, Russia.* St. Petersburg, 2008. Available at: http://lib.physcon.ru/doc?id=9531874f673b

[13] Rogovyj Je.D., Buholdin Yu.S., Levashov V.O., Martynenko G.Yu., Smirnov M.M. Patent. 77665. Ukraine (UA). MPK F16C 32/04. *Method of Discrete Magnetic Bearing Control for Revolved Rotors*. Applicant and the patentee VAT «Sum. nauk.-vyrob. ob-nja im. M.V. Frunze», Nac. tehn. un-t «Hark. politehn. in-t»; №2003076309; applicated: 08.07.03; published: 15.01.07, Bjul. №1/2007, 6.

[14] Martynenko, G. Y. *The Experimental Investigation Technique of the Dynamics of the Model Rotor in the Combined Magnetic Suspension*. Bulletin of NTU "KhPI". Series: Dynamics and strength of machines, 2013, Vol. 58(1031), p. 125-135 (in Russian).